Research on Hydrodynamic Characteristics of Axial Separation for Cross-Media Vehicles in High-Speed Underwater Environments

Xuanchen Li*, Yao Shi* and Chao Wang*
Corresponding author: cwang21@nwpu.edu.cn
* Northwestern Polytechnical University, China .

Abstract: High-speed underwater separation is a critical process for cross-media vehicles, yet the underlying unsteady hydrodynamics and multi-body interactions remain unresolved. This study numerically investigates the axial underwater separation process of a vehicle–shell system to clarify the physical mechanisms governing its hydrodynamic characteristics. A multiphase flow model utilizing the Reynolds-averaged Navier–Stokes (RANS) equations, the Volume of Fluid (VOF) method, the Schnerr–Sauer cavitation model, and an overset grid technique is established. Based on the kinematic and flow features, the separation process is systematically divided into a loading phase, an unloading phase, and a cruise phase. The effects of separation force, initial velocity, and initial water depth on the system's separation behavior are comprehensively analyzed. Results indicate that separation force is the dominant factor; a higher force significantly shortens the separation time, while an insufficient force leads to separation failure. Furthermore, a higher initial velocity prolongs the total separation time. Conversely, a lower initial velocity can induce a negative velocity state that triggers severe cavitation inside the shell. Moreover, deep-water environments generate a high ambient backpressure, which creates a sharp pressure difference that exerts a backward drag force on the shell, thereby significantly delaying the overall separation process. These findings provide valuable theoretical guidance for the design and optimization of high-speed underwater separation systems for cross-media vehicles.

Keywords: High-speed underwater separation, Multi-body interaction, Confined flow, Hydrodynamic forces.

1. Introduction

Cross-media vehicles are key systems for missions involving air, surface, and underwater environments. The safety and reliability of the water entry process directly affect mission success. High-speed underwater separation is a critical step for cross-media vehicles to traverse the air–water interface and achieve precise delivery. After high-speed water entry and effective load reduction, external protective or load-reducing structures must separate from the main vehicle in an underwater environment where the vehicle still maintains a high speed. This separation process directly affects attitude stability, motion continuity, and subsequent autonomous navigation performance.

Existing studies related to underwater separation mainly focus on underwater load release and underwater launch. For underwater load release, buoyancy release, gravity release[1], and thrust-based separation[2] are commonly used. These processes typically occur under low-speed or quasi-static conditions, and most existing studies primarily emphasize the reliability of separation devices and control strategies. Unsteady hydrodynamics, confined flow effects, and multi-body hydrodynamic interference are rarely discussed. For underwater launch, previous studies have investigated shock waves and compressibility effects under ultra-high-speed conditions[3], as well as cavitation collapse mechanisms under high-speed conditions[4]. These studies focus on the single-body motion of a vehicle launched from a static water environment under high pressure or propulsion. In contrast, underwater axial separation occurs during an established underwater cruising state. The relative motion between the vehicle and the shell

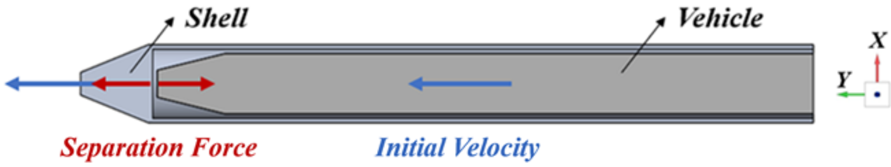

Figure 1: Physical model of axial separation

is governed by hydrodynamic interactions involving confined annular flow and multi-body coupling, which are fundamentally different from those in conventional underwater launch scenarios. Separation mechanisms in aerospace applications, such as rocket stage separation[5] and fairing separation[6], provide useful references. However, the flow–structure interaction mechanisms in underwater separation are significantly different.

Therefore, underwater separation of cross-media vehicles after high-speed water entry remains an unresolved scientific and engineering problem. In particular, the evolution of hydrodynamic loads, pressure distribution characteristics, and multi-body interaction mechanisms during separation are still not well understood. This study investigates the axial underwater separation process of a vehicle–shell system. The pressure distribution, hydrodynamic forces, and flow features during separation are analyzed. The effects of separation force, initial velocity, and water depth on separation behavior are also examined. The objective is to clarify the physical mechanisms governing high-speed axial underwater separation and to provide guidance for the design of underwater separation systems for cross-media vehicles.

2. Methodology

2.1 Numerical Modeling

The axial underwater separation model is shown in Figure 1. The shell is simplified as a hollow cylindrical structure with a conical nose, while the vehicle is simplified as a solid cylinder with a conical nose. The combined "vehicle–shell" system has already completed vertical high-speed water entry. The cavity generated during water entry has closed, and the flow field has reached a quasi-steady transient state.

At the moment of separation, the system still maintains an initial velocity. The vehicle and the shell are assumed to remain coaxial, without rotation or lateral displacement. A transient thrust device is installed between the vehicle and the shell. This device provides a short-duration separation force with a large magnitude. The thrust acts along the axial direction, driving relative motion between the vehicle and the shell. The force disappears immediately after a prescribed relative displacement.

To investigate the flow characteristics during underwater axial separation, numerical simulations based on the finite volume method are performed. The flow is modeled as a multiphase system consisting of water and vapor phases. Relative motion between the vehicle and the shell is handled using an overset grid method. This approach ensures grid stability and accuracy in the narrow annular gap during separation. The flow is governed by the Reynolds-averaged Navier–Stokes (RANS) equations. Turbulence effects are modeled using the SST k-ω model, which provides reliable predictions for both near-wall shear flows and locally separated flows. The free-surface evolution is captured using the Volume of Fluid (VOF) method. To account for possible cavitation during separation, the Schnerr–Sauer cavitation model is employed. This model describes the mass transfer between the water and vapor phases.

Figure 2 illustrates the initial contours of pressure, velocity, vorticity, and phase at the onset of separation.

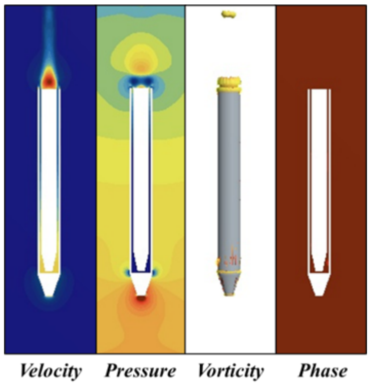

Figure 2: Contours at the initial moment

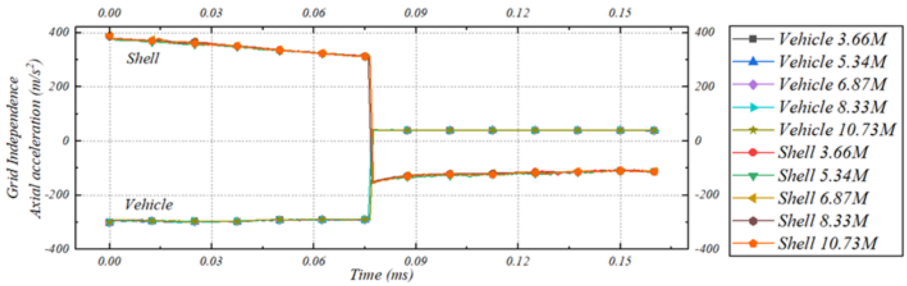

Figure 3: Grid independence verification

2.2 Numerical Modeling

Grid and time-step independence verifications are conducted for the established physical model. Five different grid resolutions ranging from 3.66 million to 10.73 million elements are tested. Taking the finest grid (10.73 million elements) as the baseline, the maximum relative errors and average errors of the vehicle and shell accelerations are evaluated. For the selected grid of 6.87 million elements, the maximum relative error of the vehicle acceleration is 2.5% with an average error of 0.59%. Meanwhile, the maximum relative error of the shell acceleration is 4.80% with an average error of 1.06%. The axial acceleration curves for these different grids are illustrated in Figure 3.

As observed from the figure above, the variation in the grid number has a minor effect on the computational results, and the shell is more sensitive to grid changes. Considering both computational accuracy and efficiency, the grid consisting of 6.87 million elements is adopted.

Meanwhile, four different time steps ranging from 1×10^{-4} s to 10×10^{-4} s are tested. Taking the smallest time step (1×10^{-4} s) as the baseline, the maximum relative errors and average errors of the vehicle and shell accelerations are evaluated. For the selected time step of 5×10^{-4} s, the maximum relative error of the vehicle acceleration is 4.43% with an average error of 0.59%. Meanwhile, the maximum relative error of the shell acceleration is 8.49% with an average error of 2.23%. The axial acceleration curves for these different time steps are illustrated in Figure 4.

Similarly, as observed from figure above, the variation in the time step has a minor effect on the computational results, and the shell is more sensitive to time step changes. Considering both computational accuracy and efficiency, a time step of 5×10^{-4}s is adopted for the calculations.

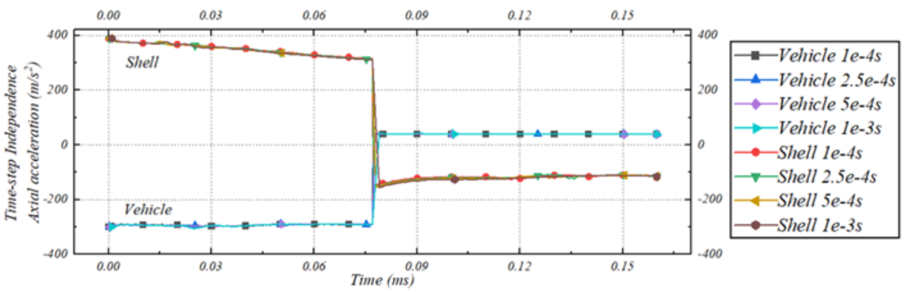

Figure 4: Time-step independence verification

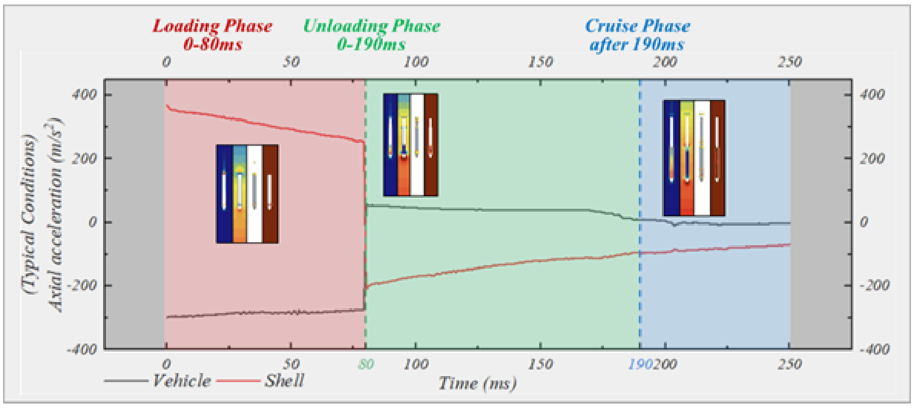

Figure 5: Stages of the axial separation process

3. Results and Discussion

3.1 Separation Process

This study systematically investigates the axial separation behavior of a vehicle during underwater cruising. The time histories of displacement, velocity, acceleration, and hydrodynamic loads are analyzed to describe the evolution of the separation process. Based on these results, the axial separation process is divided into three stages: the loading phase, the unloading phase, and the cruise phase. Representative acceleration curves and pressure contours are shown in Figure 5 and Figure 6.

The loading phase refers to the process from the initiation of separation to reaching the prescribed relative displacement. During this phase, separation thrust is continuously applied between the vehicle and the shell, driving relative axial motion. As the relative motion develops, fluid in the annular gap accelerates, generating a pronounced low-pressure region inside the shell. This low pressure then triggers cavitation,

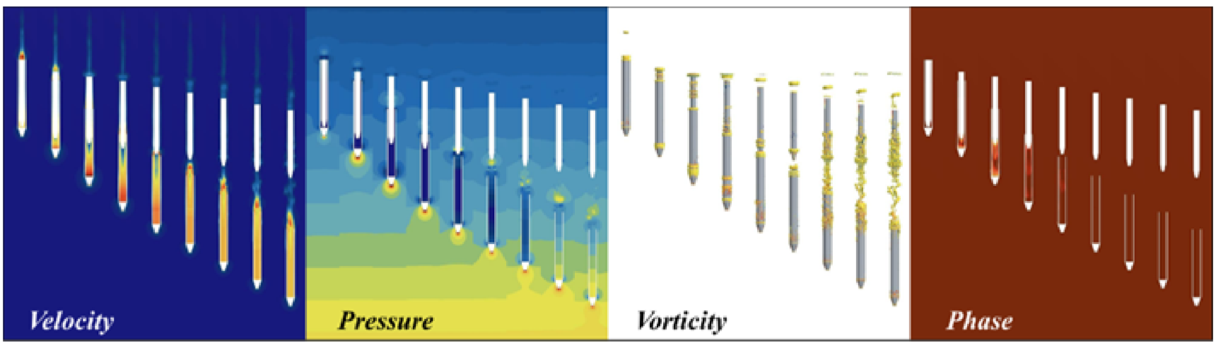

Figure 6: Flow field contours during the separation process

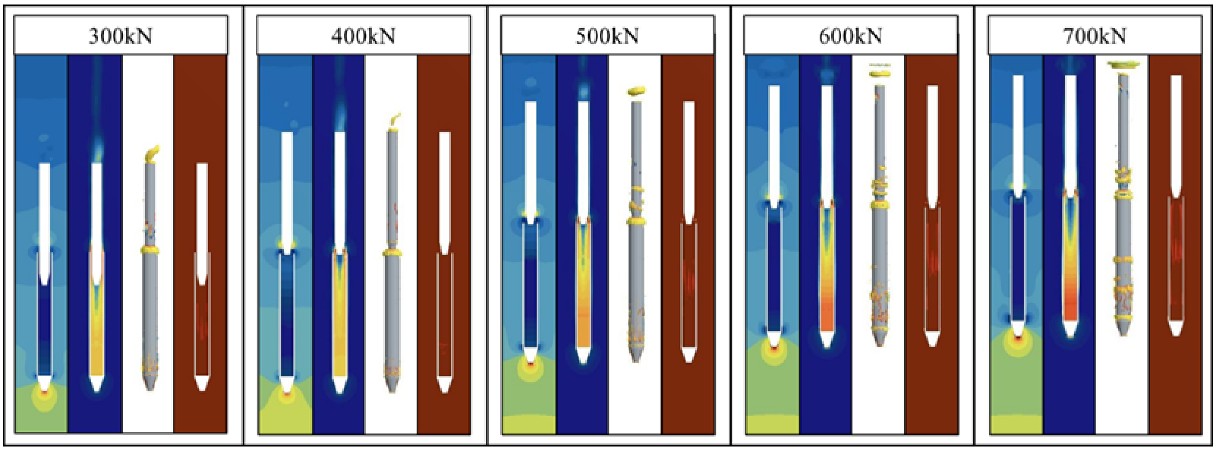

Figure 7: Contours of pressure, velocity, vorticity, and phase at the end of the unloading phase under different separation forces

which gradually intensifies over time. During this phase, the separation thrust and hydrodynamic forces act together, determining the initial dynamics of the separation process and the formation of the low-pressure environment. The unloading phase refers to the process from the cessation of separation thrust after reaching the prescribed relative displacement until the vehicle exits the shell. During this phase, no additional separation force is applied. The relative motion relies mainly on the inertia accumulated during the previous phase and continues to be influenced by hydrodynamic forces. As the relative motion continues, the fluid in the annular gap must keep adjusting to the displacement between the vehicle and the shell. The low-pressure region inside the shell begins to recover, and cavitation gradually collapses. However, because the relative motion is not yet complete, the fluid acceleration process continues. The pressure inside the shell cannot quickly return to the ambient static pressure, so the low-pressure state persists during this phase. This phase represents the transition from a separation-force-dominated process to a hydrodynamically dominated one. The cruise phase starts when the the nose of the vehicle reaches the shell tail and continues afterward. At this stage, the vehicle is largely free from geometric constraints imposed by the shell. It is mainly affected by wake interference from the shell. The vehicle enters an independent underwater cruising state, and the influence of the separation process on subsequent motion becomes stable.

3.2 Effects of Separation Force on Separation Characteristics

The separation force serves as the direct power source driving the relative motion between the vehicle and the shell. Consequently, it determines both the overall time scale and the load level of the axial separation process. An increase in the separation force reduces the durations of both the loading and unloading phases. As a result, the vehicle enters the cruise phase earlier. Specifically, under a separation force of 700 kN, the vehicle completely exits the shell and enters the cruise phase at 169 ms. However, when the force decreases to 600 kN, 500 kN, and 400 kN, the exit times are delayed to 190 ms, 223 ms, and 284 ms, respectively. This indicates that a higher separation force directly shortens the total separation time. Figure 7 illustrates the contours of pressure, velocity, vorticity, and phase at the end of the unloading phase under various separation forces:

Specifically, under a separation force of 300 kN, the vehicle fails to exit the shell by the end of the simulation due to insufficient driving force. Thus, this case is deemed a separation failure. For the conditions ranging from 400 kN to 700 kN, a higher separation force induces a greater flow velocity within the high-speed region at the front of the inner shell. Simultaneously, the low-speed region at the nose of the vehicle not only experiences a further decrease in velocity but also exhibits a significant expansion in its coverage area. Furthermore, the "suction" effect caused by the high-speed exit of the vehicle becomes more intense, leading to more pronounced cavitation at the same separation distance.

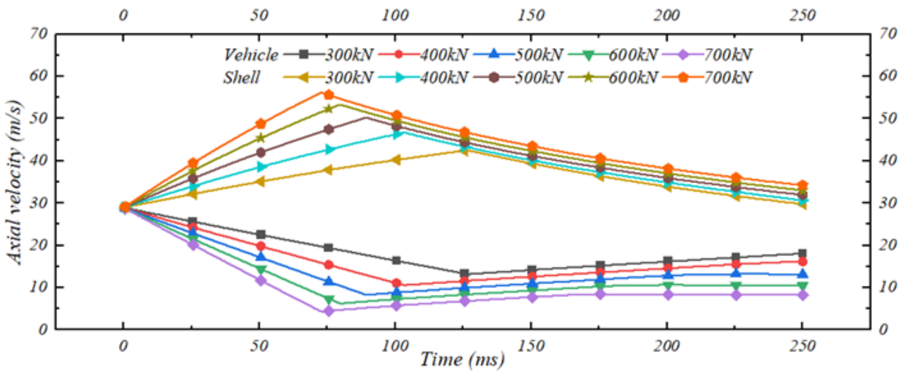

Figure 8: Velocity curves under different separation forces

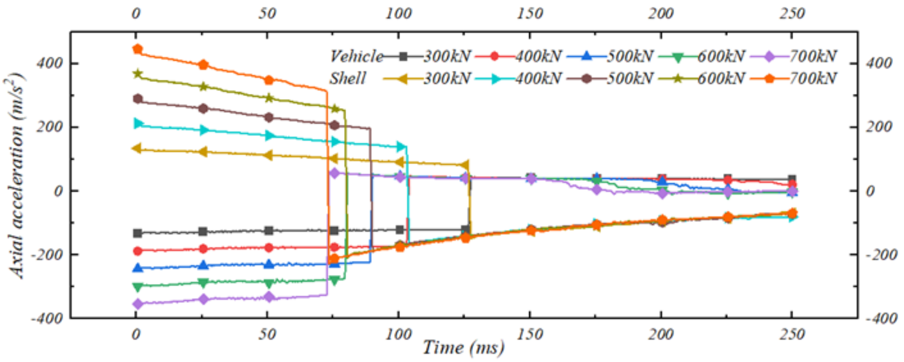

Figure 9: Acceleration curves under different separation forces

Additionally, as the separation force increases, the absolute depth at the end of the separation phase significantly decreases, thereby markedly improving the separation efficiency. The magnitude of the separation force directly determines the intensity of the kinematic response of the system during the loading phase. As indicated by the velocity and acceleration curves (Figures 8 and 9), a larger applied force yields higher peak initial axial accelerations for both the shell and the vehicle. Consequently, the velocities of the two bodies diverge sharply within an extremely short duration, which drives the system to complete the loading stroke more rapidly.

As the loading phase concludes, the system transitions into the unloading phase, during which the acceleration curve exhibits a prominent step-like decrease. At this stage, the two bodies primarily rely on the inertial kinetic energy accumulated previously to overcome the hydrodynamic drag of the ambient fluid and continue the separation process. The evolution of the velocity curves clearly indicates that an increase in the separation force significantly shortens the total duration of the loading and unloading phases. Under high-load conditions, the two bodies rapidly increase their relative displacement, enabling the vehicle to exit the shell efficiently. Conversely, under low-load conditions, the relative velocity acquired by the system is relatively small due to an insufficient initial separation driving force. Consequently, the system cannot effectively overcome the continuous hydrodynamic drag during the prolonged unloading process. As a result, the evolution of both acceleration and relative velocity gradually stagnates, and the vehicle fails to exit the shell within the expected timeframe, ultimately leading to a separation failure.

In summary, the separation force is the dominant parameter that controls the flow field evolution, kinematic characteristics, and the overall success or failure of the separation process.

3.3 Effects of Initial Velocity on Separation Characteristics

The initial velocity determines the macroscopic kinetic energy state and the initial fluid environment of the vehicle–shell system prior to separation. As the initial velocity increases, the durations required for

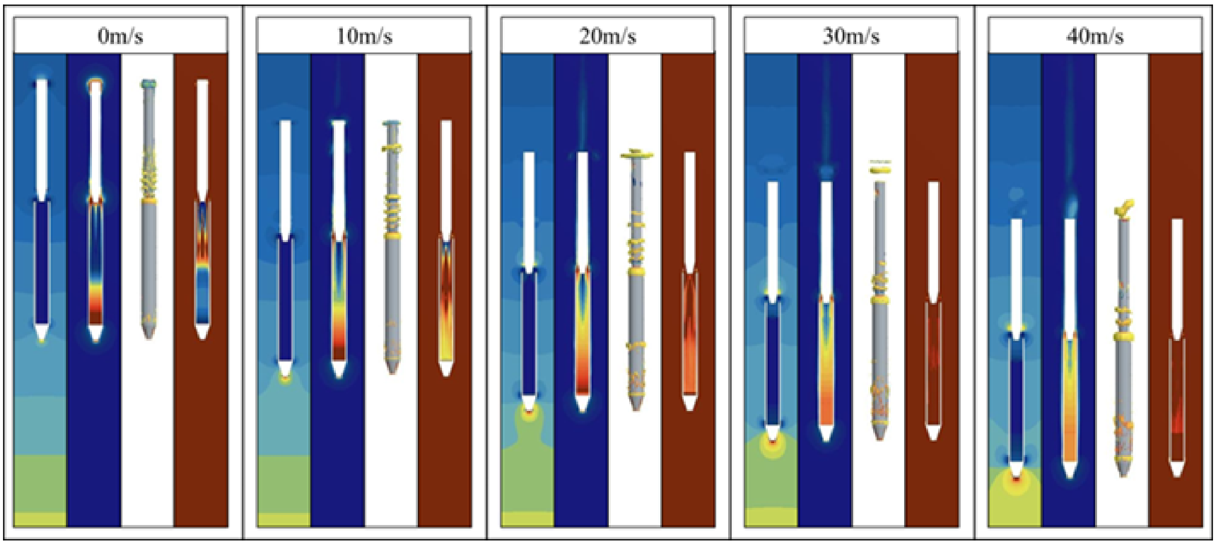

Figure 10: Contours of pressure, velocity, vorticity, and phase at the end of the unloading phase under different initial velocity

the system to complete the loading and unloading phases gradually lengthen. Consequently, the onset of the cruise phase is significantly delayed. Specifically, when the initial velocity is 0 m/s (a static water environment), the vehicle completely exits the shell and enters the cruise phase at 169 ms. However, when the velocity increases to 10 m/s, 20 m/s, 30 m/s, and 40 m/s, the exit times are delayed to 174 ms, 183 ms, 190 ms, and 204 ms, respectively. This indicates that a higher initial velocity directly leads to a longer total separation time. Figure 10 illustrates the contours of pressure, velocity, vorticity, and phase at the end of the unloading phase under different initial velocities:

As the unloading phase ends and the cruise phase begins, the fluid at the tail of the vehicle with a positive velocity can continue to shed smoothly backward. In contrast, due to the strong reverse relative motion against the surrounding flow, a large-scale, enclosing turbulent state forms on the surface of the vehicle with a negative velocity. Meanwhile, the cavitation phenomenon gradually weakens as the initial velocity increases. Specifically, the 0 m/s condition exhibits a uniquely extreme flow state. When the system possesses an initial velocity, the external ambient fluid inherently carries a relatively high incoming dynamic pressure. The fluid is not only drawn in by the negative pressure suction inside the shell but also pushed by the external dynamic pressure. Consequently, it overcomes the resistance of the narrow annular gap and fills the void left by the extracted vehicle, thereby suppressing excessive pressure drops and cavitation generation inside the shell. However, under the 0 m/s condition, the fluid outside the shell lacks any inward initial momentum. Therefore, the extremely strong enclosed suction force causes a severe global rupture of the internal fluid. This induces a highly penetrating, continuous cavitation column that extends throughout almost the entire internal space of the shell. Predictably, this will subsequently evolve into a massive cavitation collapse load, which would severely affect the kinematic states of the vehicle and the shell. As indicated by the velocity and acceleration curves (Figures 11 and 12), the initial velocity exerts a significant modulating effect on the time scale of the separation process. As the initial velocity increases, the duration required for the system to complete both the loading and unloading phases gradually lengthens.

Furthermore, the evolution of the velocity curves intuitively reveals the divergence of kinematic states induced by the initial velocity. Based on whether the absolute velocity crosses zero, these states can be classified into three categories. The first is a positive velocity state, where the cruising direction remains unchanged (30 and 40 m/s). The second is a negative velocity state, where the absolute velocity crosses zero and the direction of motion reverses (0 and 10 m/s). The third is a critical condition, where the extreme velocity approaches zero, representing the boundary of the kinematic state transition (20 m/s).

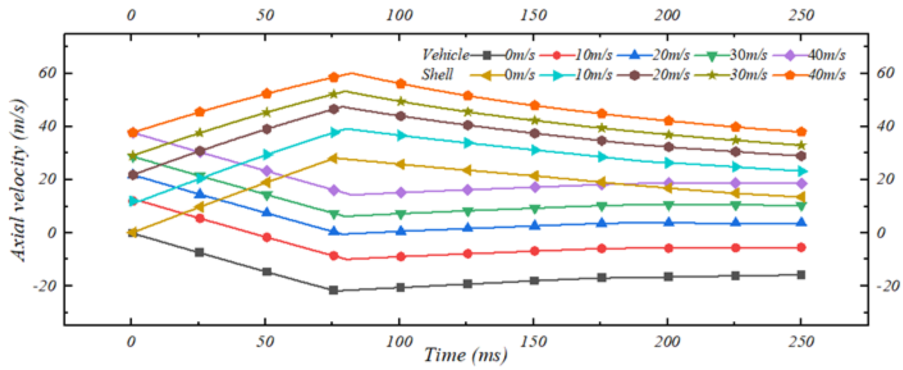

Figure 11: Velocity curves under different initial velocity

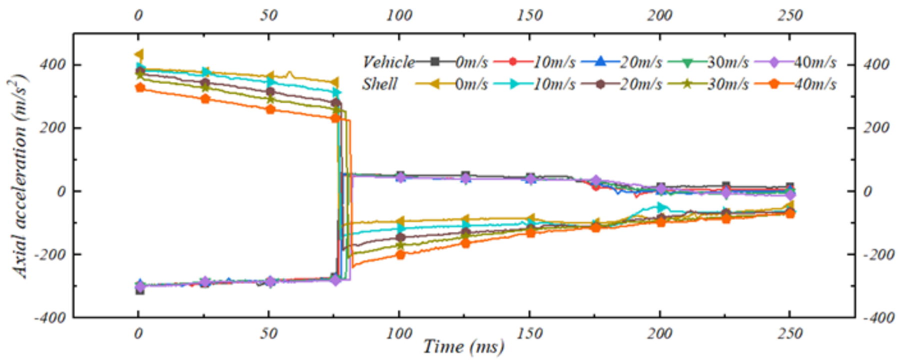

Figure 12: Acceleration curves under different initial velocity

Despite fundamental differences in their macroscopic motion directions, the acceleration curves indicate that the evolutionary characteristics of all conditions are highly consistent during the transition from the loading phase to the unloading phase. When the conical nose of the vehicle exits the shell, the physical constraints of the annular gap are suddenly released. Consequently, the accelerations of both bodies under all depth conditions exhibit a pronounced step-like sudden drop. In summary, the initial velocity affects the separation efficiency primarily by altering the initial kinetic energy of the system and the state of the surrounding fluid.

3.4 Effects of Initial Water Depth on Separation Characteristics

The initial water depth affects the axial separation process of the system primarily by altering the ambient static pressure. As the initial water depth increases, the exit time—when the system completes the unloading phase and enters the cruise phase—is gradually delayed. Specifically, at an initial depth of 15 m, the vehicle completely exits the shell at 186 ms. When the depth increases to 20 m, 25 m, 30 m, and 35 m, the exit times are delayed to 190 ms, 198 ms, 205 ms, and 207 ms, respectively. This indicates that a greater initial water depth directly leads to a longer overall separation time. Figure 13 illustrates the contours of pressure, velocity, vorticity, and phase at the end of the unloading phase under various initial water depths:

After the unloading phase concludes and the cruise phase begins, the nose of the vehicle clears the opening of the shell. This establishes a direct connection between the interior of the shell and the external water environment. At this stage, the influence of the initial water depth on the evolution of cavitation inside the shell exhibits extremely significant differences. The phase contours indicate that as the initial water depth increases, the cavitation phenomenon inside the shell weakens sharply. Under the shallow water conditions of 15 m and 20 m, the ambient static pressure is relatively low. Consequently, the backflowing external fluid is insufficient to rapidly collapse the cavity generated by the earlier suction effect, leaving a large-scale continuous cavitation region inside the shell. In contrast, as the initial water

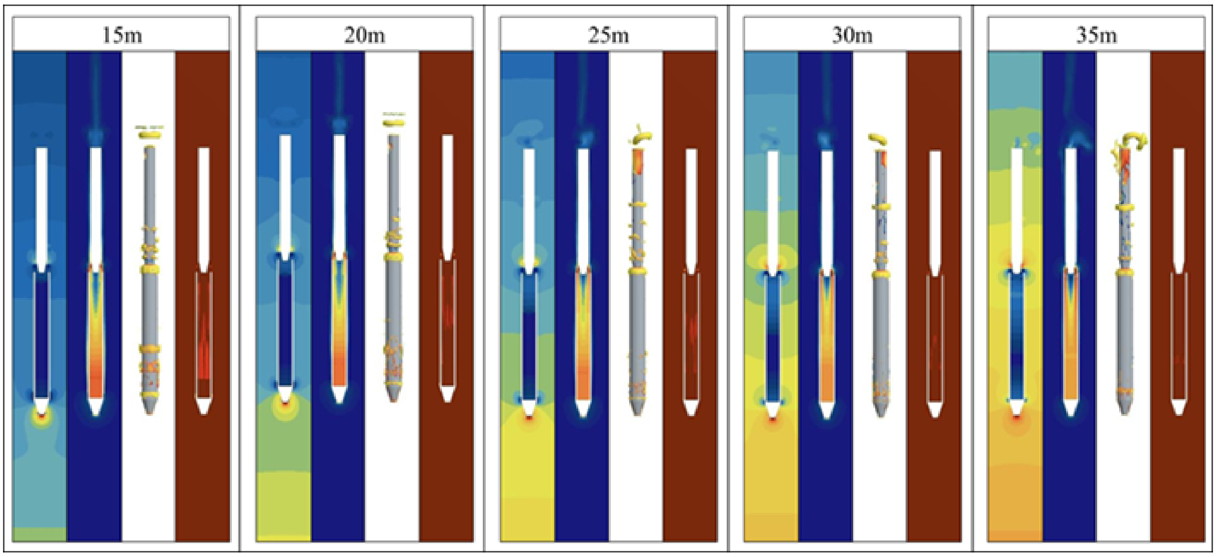

Figure 13: Contours of pressure, velocity, vorticity, and phase at the end of the unloading phase under different initial water depths

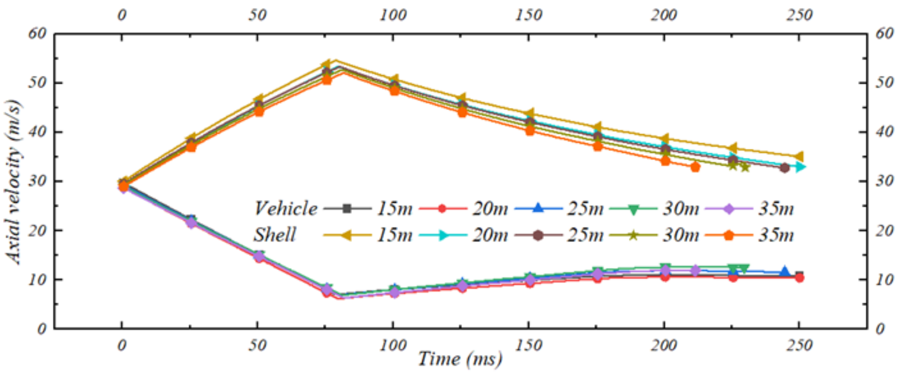

Figure 14: Velocity curves under different initial water depths

depth increases to 30 m and 35 m, the significantly higher ambient static pressure drives the external fluid to rapidly flow back into the shell. This causes the internal cavitation to be almost entirely suppressed or collapsed, allowing the flow field to quickly recover to a pure liquid state. As indicated by the velocity and acceleration curves (Figures 14 and 15), the variations in the velocity and acceleration of the vehicle are not closely correlated with changes in the water depth. In contrast, the kinematic state of the shell is relatively sensitive to the ambient static pressure. During the high-speed separation process, the extraction of the vehicle creates a low-pressure region inside the shell that drops below the saturated steam pressure. Prior to the collapse of the cavities, the internal pressure is essentially maintained near this saturated steam pressure. As the absolute water depth increases, the ambient static backpressure continues to rise. This causes the pressure difference between the inside and outside of the shell to increase sharply. This immense pressure difference generates a force that drags the shell backward. Therefore, a greater water depth results in a lower absolute velocity acquired by the shell during the loading and unloading phases. This directly suppresses the relative separation velocity between the two bodies in deep-water environments. Consequently, at greater water depths, the moment when the vehicle completely escapes the physical constraints of the shell is significantly delayed. In summary, the initial water depth influences the pressure difference between the inside and outside of the shell by altering the ambient pressure, thereby affecting the separation efficiency.

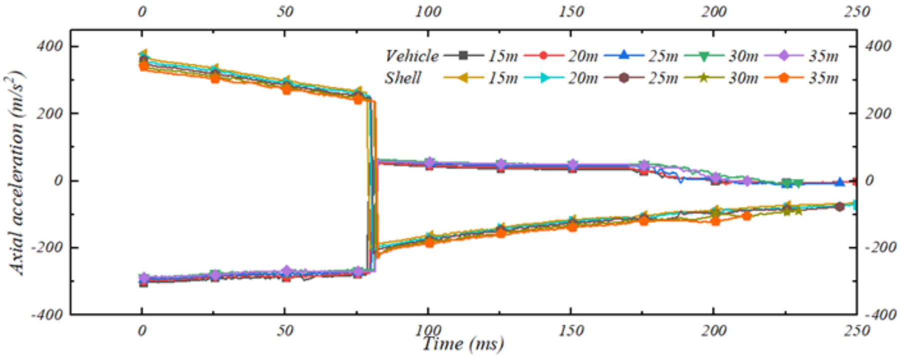

Figure 15: Acceleration curves under different initial water depths

4. Conclusion

Focusing on the high-speed axial underwater separation process of cross-media vehicles, this study describes the entire separation process in stages based on its physical characteristics. Furthermore, it investigates the effects of three key parameters—separation force, initial velocity, and initial water depth—on the separation behavior, thereby clarifying the evolution mechanisms of the separation process and the parameter regulation mechanisms. The main conclusions are as follows:

Before the vehicle completely escapes the physical constraints of the shell, the axial separation process can be primarily divided into a separation-force-dominated loading phase and an inertia- and hydrodynamically-dominated unloading phase. When the conical nose of the vehicle exits the shell and the physical constraints of the annular gap are released, the separation process enters the cruise phase.

Increasing the separation force enables the shell and the vehicle to attain extremely high peak initial axial accelerations. This causes the velocities of the two bodies to diverge rapidly within an extremely short period, thereby significantly reducing the total time required for the loading and unloading phases and improving the separation efficiency. Conversely, if the separation driving force is insufficient, the system cannot effectively overcome the continuous hydrodynamic drag.

A higher initial velocity results in a slower divergence of relative velocity at the same time nodes, thereby prolonging the total time required for the system to complete the separation. Furthermore, differences in the initial velocity directly lead to a divergence in the kinematic trajectory of the vehicle. This causes the vehicle to exhibit either a "positive velocity state," where it continuously moves forward, or a "negative velocity state," where its direction of motion reverses during the separation stroke. The negative velocity state often induces severe cavitation inside the shell, which adversely affects the separation of the vehicle and its subsequent stability.

The velocity response of the vehicle is not significantly affected by water depth, whereas the kinematic state of the shell is relatively sensitive to ambient pressure. Because an extremely low negative-pressure region exists inside the shell during the separation process, the high backpressure in a deep-water environment causes the pressure difference between the inside and outside of the shell to increase sharply. This generates a backward drag force, causing the absolute velocity of the shell to decrease as the depth increases. This deceleration of the shell directly suppresses the relative separation velocity between the two bodies, resulting in a significant delay in the overall separation time under deep-water conditions.

Acknowledgements

This study was funded by the National Natural Science Foundation of China (Grant No. U2341285)

References

[1] J Song, H Shen, et al. Design and CFD simulation analysis of a multistage separable AUV. The Ocean Engineering, 37(5):107-117, 2019.

[2] B Song, C Shao, et al. A New Method of Load Separation from Autonomous Underwater Vehicle. Acta Armamentarii, 28(2):249-252, 2007.

[3] J Zhang, Y Yu, et al. Numerical investigation of a muzzle multiphase flow field using two underwater launch methods. Defence Technology, 18(8):1454-1469, 2022.

[4] Y Wang, C Huang, et al. On the internal collapse phenomenon at the closure of cavitation bubbles in a deceleration process of underwater vertical launching. Applied Ocean Research, 56:157-165, 2016.

[5] C Ma, S Wang, J Yu. Numerical Study on the Influence of Separation Time Sequence on the Initial Thermal Separation. Energies, 17(7):1598, 2024.

[6] H Kasahara, A Matsuo .Three-Dimensional Numerical Investigation of Hypersonic Projectile Launched by Railgun on Transitional Ballistics. Journal of Spacecraft and Rockets, 58(4):919-935, 2021.